Temperature-insensitive Mach-Zehnder interferometric strain sensor based on concatenating two waist-enlarged fiber tapers

Feng Xu (徐 峰)[*], **Can Li (李 灿), Dongxu Ren (任东旭), Lu Lu (卢 璐), Weiwei Lü (吕卫卫),**
Fei Feng (冯 飞), and Benli Yu (俞本立)

School of Physics and Materials Science, Anhui University, Hefei 230039, China
[*]*Corresponding author: fengx@ahu.edu.cn*

A novel temperature-insensitive strain sensor, based on an in-line Mach-Zehnder interferometer, is fabricated by concatenating two waist-enlarged fiber tapers separated by a short piece of photonic crystal fiber. The interference spectrum of the proposed sensor is analyzed in detail. Experimental results demonstrate that this sensor has a strain sensitivity of 3.02 pm/$\mu\varepsilon$ and maintains the temperature insensitivity feature. The proposed sensor has great potential in diverse sensing applications due to its advantages, such as its compact size, low cost, and simple fabrication process.

OCIS codes: 060.2310, 060.2370.
doi: 10.3788/COL201210.070603.

In-line fiber-optic Mach-Zehnder (MZ) interferometric sensors have attracted great interest due to their unique advantages, including their compact size, low cost, high sensitivity, immunity to electromagnetic interference, and ruggedness even in corrosive and other harsh environments[1−4]. The operating principle of the MZ sensors is based on inter-modal interference, which arises from the phase difference between the involved interfering modes, primarily including the core mode and cladding modes excited in the sensing fiber. Thus far, a number of in-line fiber-optic MZ interferometric sensors based on various configurations have been reported in the literature. To excite cladding modes or couple the core mode to cladding modes, many different methods are employed to construct such sensors, including long period gratings (LPGs)[5−7] and mismatched or misaligned core diameter and fiber tapers[8−14]. Based on the abovementioned methods, these sensors show good performance in the applications of sensing temperature, strain, bending, and refractive index. However, one constant drawback of these sensors is the cross-interference between different measurands, such as a strain sensor with an undesirable thermal sensitivity. To address this issue one has to design sensing heads with athermal packages or simultaneously and independently measure strain and temperature; however, this always increases the complexity of the sensor and seriously limits the practical application of the fiber sensor.

In this letter, we propose and experimentally demonstrate a novel in-line MZ interferometric sensor, which is formed by splicing a piece of photonic crystal fiber (PCF) between two pieces of a conventional single-mode fiber (SMF). A waist-enlarged fiber taper, which possesses much better physical strength than the waist-reduced taper, is introduced into our proposed structure (Fig. 1). At the first splicing point, the core mode of the lead-in SMF excites the cladding modes, in which a taper region formed by air holes collapse in PCF, and then couple back

into the lead-out SMF after the second splicing point. Consequently, the light from the lead-out SMF shows an interference pattern with a fringe contrast of more than 15 dB. The experimental result demonstrates that the proposed sensor has a strain sensitivity of 3.02 pm/$\mu\varepsilon$ to the axial strain. It also maintains the temperature-insensitive feature. Furthermore, this type of sensor has a much more compact size than other PCF-based sensors due to the shorter length of the PCF in our proposed configuration.

The proposed MZ interferometric sensor shown in Fig. 1 is formed by splicing a short piece of index-guiding PCF (YOFC, endless single-mode PCF) in between two SMFs (Corning, SMF-28). The PCF has a pure silica core, which is formed by removing the central air hole, and a cladding composed of five-ring air holes arranged in a hexagonal pattern. The diameters of the air holes and the entire solid region are 3.75 and 7.5 μm, respectively. The fabrication of the proposed sensor only involves cleaving and fusion splicing, which means that only common fiber-optic instruments are required to fabricate such a sensor. A waist-enlarged fiber taper plays the role of exciting the cladding modes in this structure. After the propagating mode of the lead-in SMF enters the first waist-enlarged fusion region—where the air holes are fully collapsed—the modal field is broadened due to the diffraction in the collapsed region. As a result, the enlarged mode pene-
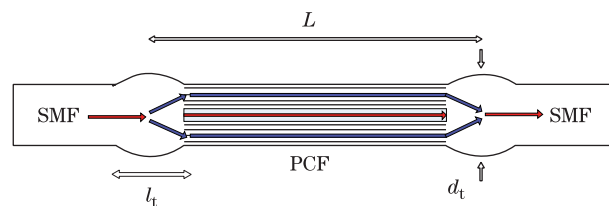

Fig. 1. Sketch of the proposed MZ interferometric sensor with waist-enlarged fiber taper.

trates into a zone of tapered voids and excites several cladding modes. These cladding modes enter the PCF and travel a short optical path along the sensing segment, finally re-coupling back to interfere with the core mode at the second splicing point.

A fusion splicer (Fujikura FSM-60s) was used to fabricate such a sensor. A short piece of PCF, unjacketed with a polymer coating, was spliced towards the lead-in/out SMFs in a manual mode. Although the splicer did not have a special project for splicing SMF to PCF, we chose the suitable splicing parameters to conduct the splicing process. To form a waist-enlarged fiber taper, the splice parameters chosen were as follows: a pre-fuse time of 200 ms, discharge electric intensity fixed at a "standard-20 bit," and the "overlap" set at 140 μm for fusion splicing. Such a fusion power ensures that the air holes of the PCF will completely collapse at a limited region, and that a large "overlap" will form a waist-enlarged fiber taper by pushing the fiber tips together. Figure 2(a) shows the side view of the formed fiber taper with a waist diameter (d_t) of $\sim$165 μm and a taper length (l_t) of $\sim$265 μm. The length of the collapsed zone was measured at $\sim$100 μm. Figures 2(b) and (d) represent the cross-sections of SMF and PCF, respectively, obtained by the microscope at the same magnification. The cross-sections of the waist-enlarged fiber tapers are presented in Figs. 2(c) and (e), which respectively show that the cross-sections of PCF and SMF located close to the taper waist have been enlarged, and that the air holes of PCF have fully collapsed under our experimental splicing conditions. Furthermore, we chose the "overlap" distance and arc discharge intensity to fabricate various tapers with different waist diameters and taper lengths. Finally, a MZ interferometric sensor was constructed by concatenating two waist-enlarged fiber tapers. Figure 2(f) shows the experimental setup for this sensor, which has been fabricated through the aforementioned method. Light from a tunable laser source with wavelength range of 1 496−1 640 nm was incident to the lead-in fiber, and the interference spectrum of the lead-out fiber was recorded by a high-accuracy lightwave measurement system (LMS, Agilent 8164A) at a resolution of 1 pm.

As mentioned above, the interference spectrum depends on the optical path difference between the two interferometric arms. Although the physical lengths of the interferometer arms are exactly the same, the interference spectrum is directly related with the effective index difference between the involved interfering modes.

Assuming that only two modes are involved in the interference, the accumulated phase difference φ between them can be given as

$$\varphi = 2\pi\Delta nL/\lambda, \qquad (1)$$

where Δn is the effective index difference between the interfering modes, L is the physical length of the interferometer, and λ is the wavelength in a vacuum. The transmission as a function of the wavelength is given as

$$T(\lambda) = I_1(\lambda) + I_2(\lambda) + 2\left[I_1(\lambda)I_2(\lambda)\right]^{1/2}\cos\left(2\pi\Delta nL/\lambda\right), \qquad (2)$$

where $I_1(\lambda)$ and $I_2(\lambda)$ are the intensities of the two interfering modes, respectively. The wavelength spacing $\Delta\lambda$

of the interference spectrum is given as

$$\Delta\lambda = \frac{\lambda^2}{\Delta n \cdot L}. \qquad (3)$$

Therefore, the interference pattern changes as the sensing fiber length changes, resulting from an external axial strain applied to the sensor. As such, we can monitor the shift of the interference peak or dip to measure the strain.

To analyze the mode interference, varied samples possessing different PCF lengths between the two tapers were fabricated. The typical transmission spectra at the PCF lengths of L_1=14 mm and L_2=22.5 mm are shown in Fig. 3(a). Both interference fringes are not uniform, but look as if they have several frequency components in the interference fringe periods. Through the collapsing method, it is easier to excite more than one cladding mode compared with the splicing method, which can introduce the mode field diameter (MFD) mismatch between the two fibers. Therefore, the inhomogeneous pattern results from several cladding modes involved in the interference. Furthermore, we also note that multiple cladding modes can be excited regardless of the taper shape. Thus, we assume that the multiple cladding modes are excited by the MFD mismatch between the two fibers. Indeed, the taper shape affects the interference fringe contrast, which benefits the resolution of the sensor. On the contrary, the maximum of fringe contrast changes slightly as PCF length increases from 14 to 22.5 mm. Thus, we can optimize the waist diameter and the taper length to obtain a sensor with a high fringe contrast. The maximum of fringe contrast fabricated in our
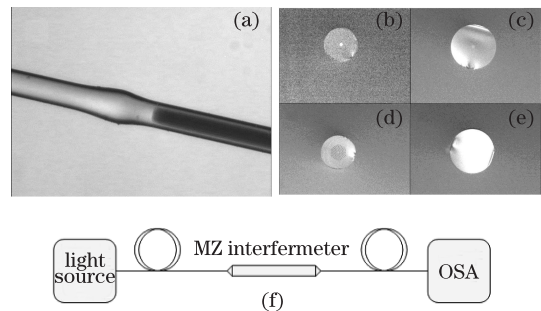

Fig. 2. (a) Side view of a waist-enlarged fusion taper (the right fiber is PCF); cross-sections for (b) SMF and (d) PCF; cross-sections of (c) SMF and (e) PCF close to the taper waist; (f) experimental setup for the proposed MZ interferometric sensor.
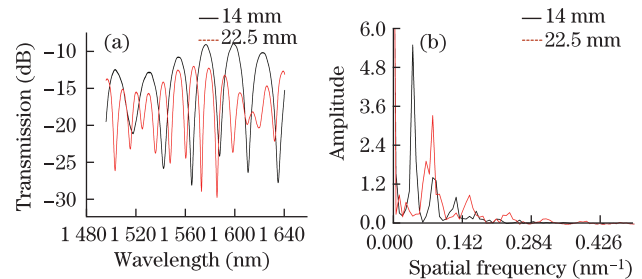

Fig. 3. (Color online) (a) Transmission spectra of the MZ interferometric sensors with different PCF lengths, L_1= 14 mm (black curve) and L_2= 22.5 mm (red curve); (b) spatial frequency spectra by taking the FFT.

experiment achieved more than 15 dB, which is better than those of all PCF-based sensors, thereby indicating that such a sensor can perform with a higher resolution.

To determine the number and power distribution of the interfering modes, the transmission spectra in Fig. 3(a) was transformed using the fast Fourier transform (FFT) method. The corresponding spatial frequency spectra are shown in Fig. 3(b). There are several peaks in the spatial frequency spectra at two PCF lengths, confirming that several cladding modes should be excited and can interfere with the core mode. However, only one cladding mode is dominantly excited, while the other cladding modes are weak, as observed from the intensity of the peaks shown in Fig. 3(b). As shown in Fig. 3(b), the spatial frequency corresponding to the dominant peak increases with the increase of the PCF length, which is similar to the results in Ref. [10]. Furthermore, Fig. 3(b) shows that at a fixed PCF length, the strongly excited cladding mode tend to be the low-order mode; this is commensurate with the fact that the spatial frequency is proportional to the differential modal group index, which in turn, is a result of the higher order cladding mode having the lower effective index or the higher differential effective index.

We tested the axial strain response of the MZ interferometric sensor with PCF length of 14 mm, which has a higher fringe contrast compared with the other sensors. Figure 4(a) shows the interference fringe changes with different strains at a fixed wavelength of 1 565.5 nm. From Fig. 4(a), one can see that the center of the dip shifts to the short wavelength with the increase of the strain. The strain-induced variations of the interference fringes were obtained with a small step increment of the strain, and then plotted in Fig. 4(b). The wavelength is linearly proportional to the axial strain with a strain sensitivity of 3.02 pm/$\mu\varepsilon$, which is higher than the typical sensitivity of the Bragg grating-based strain sensors ($\sim$1.1 pm/$\mu\varepsilon$).
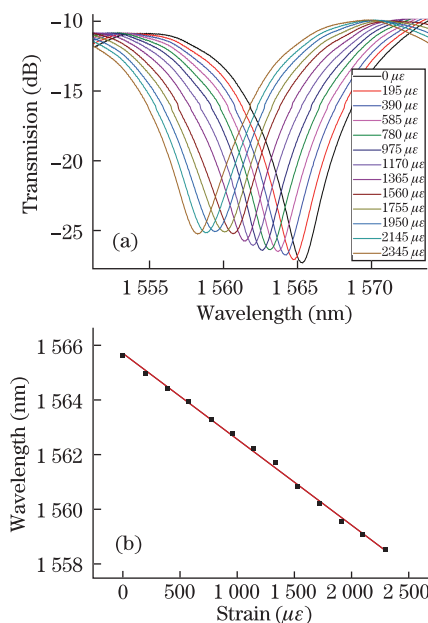

Fig. 4. (a) Fringe dip shifts with the increase of axial strain at the wavelength of 1 565.5 nm, and (b) the axial strain sensitivity.
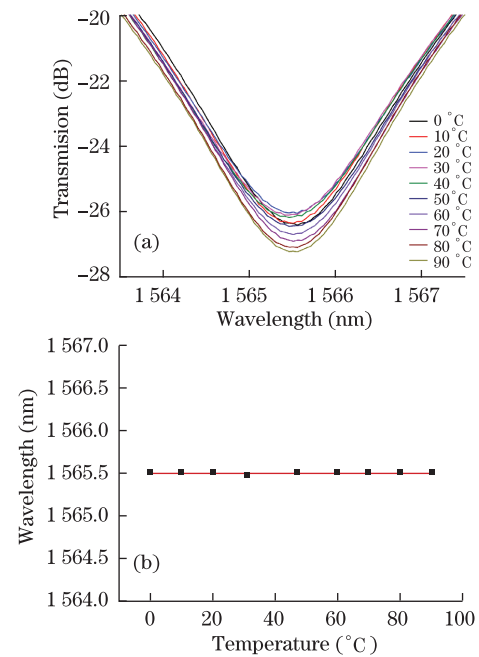

Fig. 5. (a) Fringe dip shifts with the increase of temperature at the wavelength of 1 565.5 nm, and (b) the temperature sensitivity.

We investigated the temperature response of the proposed MZ interferometric sensor. The entire sensing part was mounted in a glass capillary tube and kept straigh during heating in a temperature chamber. The intensity of the dip, recorded at wavelength of 1 565.5 nm, changed as the temperature increased from 0 to 90 °C as shown in Fig. 5(a). However, the central wavelength of the dip does not move as the temperature changes. Such a sensor shows temperature insensitivity, due to the PCF structure with air holes, making it the best candidate for the temperature-insensitive strain sensor[15]. Therefore, the temperature compensation is not necessary if such a sensor is operated in a normal environment.

In conclusion, we propose and experimentally demonstrate an in-line MZ interferometric sensor by splicing a piece of PCF in between two SMFs. The collapsing region, with a waist-enlarged fiber taper, excites multiple cladding modes and results in the inter-modal interference between the core mode and the cladding modes. The proposed strain sensor device has many advantages, such as a perfectly linear response with a strain sensitivity of $\sim$3.02 pm/$\mu\varepsilon$, temperature insensitivity, good physical strength, and a simple fabrication process. The MZ interferometric sensor can be used in varied applications in the field of fiber sensing.

References

1. O. Frazao, P. Caldas, F. M. Araujo, L. A. Ferreira, and J. L. Santos, Opt. Lett. **32,** 1974 (2007).

2. Y. Liu and L. Wei, Appl. Opt. **46,** 2516 (2007).

3. F. Pang, W. Liang, W. Xiang, N. Chen, X. Zeng, Z. Chen, and T. Wang, IEEE Photon. Technol. Lett. **21,** 76 (2009).

4. T. Zhao, Y. Gong, Y. Rao, Y. Wu, Z. Ran, and H. Wu, Chin. Opt. Lett. **9,** 050602 (2011).

5. C.-Y. Lin, L. A. Wang, and G.-W. Chern, J. Lightwave Technol. **19,** 1159 (2001).

6. Y. Lin, J. A. R. Williams, and I. Bennion, IEEE Photon. Technol. Lett. **12,** 531 (2000).

7. J. H. Lim, H. S. Jang, K. S. Lee, J. C. Kim, and B. H. Lee, Opt. Lett. **29,** 346 (2004).

8. L. V. Nguyen, D. Hwang, S. Moon, D. S. Moon, and Y. Chung, Opt. Express **16,** 11369 (2008).

9. B. Dong, D.-P. Zhou, L. Wei, W.-K. Liu, and J. W. Y. Lit, Opt Express **16,** 19291 (2008).

10. H. Y. Choi, M. J. Kim, and B. H. Lee, Opt. Express **15,** 5711 (2007).

11. B. Dong, D.-P. Zhou, and L. Wei, J. Lightwave Technol. **28,** 1011 (2010).

12. Z. Tian, S. S.-H. Yam, J. Barnes, W. Bock, P. Greig, J. M. Fraser, H.-P. Loock, and R. D. Oleschuk, IEEE Photon. Technol. Lett. **20,** 626 (2008).

13. P. Lu, L. Men, K. Sooley, and Q. Chen, Appl. Phys. Lett. **94,** 131110 (2009).

13. Z. Tian and S. S.-H. Yam, IEEE Photon. Technol. Lett. **21,** 161 (2009).

14. P. Lu, L. Men, K. Sooley, and Q. Chen, Appl. Phys. Lett. **94,** 131110 (2009).

15. M. Deng, C.-P. Tang, T. Zhu, and Y.-J. Rao, Opt. Commun. **284,** 2849 (2011).